Interaction and Multiscale Mechanics, Vol. 2, No. 1 (2009) 1-14
DOI: http://dx.doi.org/10.12989/imm.2009.2.1.001

Interaction fields based on incompatibility tensor in field theory of plasticity-Part I: Theory-

Tadashi Hasebe*

Kobe University, Rokkodai, Nada, Kobe 657-8501, Japan

(Received March 23, 2008, Accepted August 15, 2008)

Abstract. This paper proposes an interaction field concept based on the field theory of plasticity. Relative deformation between two arbitrary scales, e.g., macro and micro fields, is defined which can be implemented in the crystal plasticity-based constitutive framework. Differential geometrical quantities responsible for describing dislocations and defects in the interaction field are obtained, based on which dislocation density and incompatibility tensors are further derived. It is shown that the explicit interaction exists in the curvature or incompatibility tensor field, whereas no interaction in the torsion or dislocation density tensor field. General expressions of the interaction fields over multiple scales with more than three scale levels are derived and implemented into the present constitutive equation.

Keywords: multiscale modeling; crystal plasticity; field theory; differential geometry; non-Riemannian plasticity.

1. Introduction

Developments of realistic and practically feasible multiscale modeling and simulations in polycrystalline plasticity of metallic materials have been highly expected for a long time, however, we must admit that we are still at a primitive stage, in the sense that many researchers seem to have tried to capture the related subjects in quite reductionistic way without looking into the real complexities underlying them. It may safely be said that boundless demands for the computational power and pursuits of larger-scale massively parallelized simulations relying largely upon the brutal forces would be the indications of such trend. Huge amount of experimental data accumulated to date, on the other hand, strongly requires us to proceed to the "next stage" multiscale modeling and simulation of materials beyond such reductionistic perspectives. Since polycrystalline metallic materials can be regarded as one of the simplest examples of complex systems, where concurrently interacting inhomogeneities in distinctively multiple spatiotemporal scales accompanied by associated feedback loops substantially control the mechanical properties, what we definitely and urgently need should be the construction of theoretical frameworks and methodologies that can allow us to deal with them in an appropriate manner. We must also recognize the importance of inhomogeneously deforming fields in multiple scales, e.g., dislocation substructures evolving into sub-micrometer ordered patterns, intra-granular deformation structures such as lamellar bands and

* E-mail: hasebe@mech.kobe-u.ac.jp

those associated with collective behavior of crystal grain assemblage, most of which are averaged out macroscopically. No one has clarified hitherto, however, what the interactions among them on earth and their essential roles are as well in conspiring to dictate the mesoscopic and macroscopic mechanical responses of complex kinds.

Homogenization method (e.g. Benssousan *et al*. 1978, Terada and Kikuchi 2001) is a mathematically well-established scheme applicable to such coupling problems, however, its applicability is limited basically to the case with completely separable scales where the scale ratio must tend to zero, in addition to the rigid prerequisite of the periodicity of the assumed microstructure to be dealt with. Furthermore, the effects from the microscale are reflected via perturbation to the macro-field in this framework, whose shortcomings is that the phase transition-like phenomena cannot be described, i.e., the evolution of the system to be dealt with is always limited within the non-singular response. These drawbacks will be a fatal impediment to accomplish the above-mentioned ambition over the multiscale modeling.

Another open question of immense significance is how to describe the "inhomogeneites" in various scales. In the homogenization method, such spatial information is numerically modeled via direct discretization, e.g., by utilizing FEM. This seems to be convenient and effective; however, we also need mathematically tractable way for more general treatments of the inhomogeneities that can be easily extended to multiple scale interactions. For describing the inhomogeneities in a generalized sense, an effective as well as rational use of the differential geometrical language has been attempted by the author (Hasebe 2004a, 2004b, 2006) based on the unique framework known as "non-Riemannian plasticity" (Kondo 1955). In particular, the prominent features of the incompatibility tensor, given by second gradient of strain, have been clarified in the present context (Hasebe 2006, Aoyagi and Hasebe 2007). Another use of differential geometry along somewhat different lines has been proposed (Epstein and Elzanowski 2007) also for describing the inhomogeneities, where Eshelby stress is regarded as a candidate for the "driving force" responsible for the field evolutions. The next important step for us to take is to develop a method to rigorously describe the interplay among the inhomogeneities in multiple scales, which will also contribute to the field evolutions.

This paper intends to construct a mathematical framework for describing the interplay among multiple-scale inhomogeneities based on the differential geometrical field theory. A detailed derivation process of the two-scale interaction and its interpretation together with the extension to multiple scales are provided, after giving a brief review of the differential geometrical quantities followed by a new intuitively tangible physical image of the incompatibility tensor field which is responsible for the inhomogeneous field descriptions. Application examples of the three-scale interaction field formalism constructed here will be given in Part II of the present paper (Hasebe 2009).

2. Theory of interaction fields

2.1 About differential geometrical field theory

Since the differential geometrical descriptions of dislocations and defects have been well-documented (e.g. Kondo 1955, Amari 1962), here we will encapsulate the intuitive images and the definitions of them. Fig. 1 presents schematics of primitive physical images of "torsion" and

"curvature" of a crystalline space in terms of plasticity, both of which are expressed via higher rank tensors based on differential geometry. By using the two quantities, we can thoroughly express all kinds of imperfections in principle (Kondo 1955, Ohnami 1988). The "torsion," characterized by a closure failure of the circuit enclosing the defected field, i.e., known as Burgers vector, accounts for the one-signed dislocations, while the "curvature," featuring imperfections accompanied by the rotation of material vector during encircling the field, expresses not only pairs of dislocations like dislocation dipole and multi-poles but also other kinds of defects including vacancy, foreign atoms, and precipitates.

Torsion and curvature tensors are defined by,

$$S_{kl}^{\cdot\cdot j} = \Gamma_{[kl]}^{j}$$

$$R_{klm}^{\cdots n} = 2[\partial_{[k}\Gamma_{l]m}^{n} + \Gamma_{[k|p|}^{n}\Gamma_{l]m}^{p}] \tag{1}$$

respectively, where Γ_{kl}^{j} indicate the coefficients of connection in non-Riemannian space. Contractions of these higher order tensors considering the symmetry lead to well-known second rank tensors. They are called "dislocation density tensor" and "incompatibility tensor," respectively, further given by a curl of distortion tensor and double curl of strain tensor in the context of continuum mechanics, i.e.,

$$\alpha_{ij} = -\in_{ikl}\partial_k\beta_{lj}^{p} = \frac{1}{2}\in_{ikl}S_{kl}^{\cdot\cdot j}$$

$$\eta_{ij} = \in_{ikl}\in_{jmn}\partial_k\partial_m\varepsilon_{ln}^{p} = \frac{1}{4g}\in_{ikl}\in_{jmn}R_{klm}^{\cdots n} \quad (g = \det(g_{ij})) \tag{2}$$

This means that the theory intrinsically requires "strain gradients" at least up to the second order as far as the present framework is concerned. Note, another definition or interpretation of the incompatibility tensor is the Einstein tensor derivable from the 4th rank, $R_{lij}^{\cdots k}$

$$\eta_{ij} = R_{ij} + \frac{1}{2}Rg_{ij} \tag{2a}$$

where $R_{ij} \equiv R_{inj}^{n}$ is the Ricci curvature and $R \equiv g^{ij}R_{ij}$ is called the scalar curvature. Here, g_{ij} or g^{ij} represents the metric tensor of the space, which measures the strain in the field theory. Also η_{ij} can be rewritten in terms of the gradient of α_{ij}, i.e.,

$$\eta_{ij} = -(\in_{ikl}\partial_k\alpha_{jl})_{sym} \tag{2b}$$

where "*sym*" stands for the summarization with respect to *i* and *j*.

2.2 Intuitive physical image of incompatibility tensor-driven inhomogeneity evolution

The torsion and curvature tensors defined above can play pivotal roles in describing not only dislocation and defect fields but also generalized inhomogeneously deforming fields in any scale levels, e.g., dislocation substructures in grain size orders and stress supporting structure in grain-aggregate orders. Since the inhomogeneous fields are evolved ultimately as a consequence of motions and interactions of crystallographic imperfections including both dislocations and defects, their generalized physical images are also attributed ultimately to the redistributions of dislocations

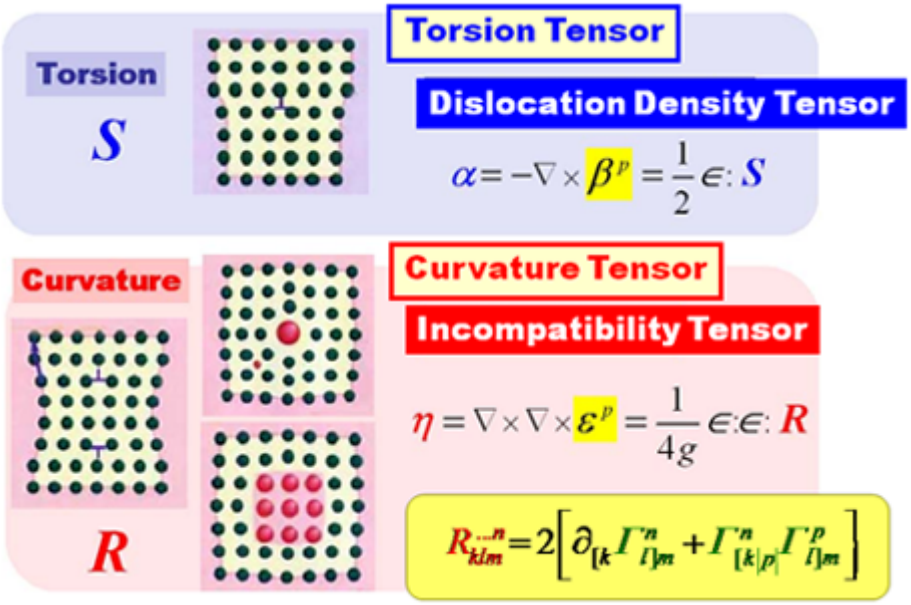

Fig. 1 Differential geometrical quantities for describing crystal imperfections via torsion and curvature tensors, further reduced to dislocation density and incompatibility tensors by contractions, respectively

and defects.

Introducing the incompatibility tensor to, e.g., the hardening law, in an "appropriate" manner as detailed in section **4** has been demonstrated to soften the overall response, associating with additionally introduced "modulations" in the deformation field (Aoyagi and Hasebe 2007). This stems from supplementary accommodation mechanisms to be embodied by the incompatibility field. An intuitive physical image of this accommodation process is given in Fig. 2, schematizing a dislocation rearrangement into a kink band configuration as one of the possibilities. When a region of a material is subject to localized shear (right-hand side of Fig. 2(a)), a non-uniform plastic deformation should be introduced resulting in localized strain gradient at around the interfacial region between before and after the passage of one-signed dislocations, producing locally "incompatible" deformation. Fig. 2(b) illustrates the corresponding "virtual" configuration, which is conventionally interpreted as being compensated by the "geometrically-necessary" dislocations (e.g. Fleck and Hutchinson 1997). To lower the strain energy of the whole system, however, further rearrangement of the dislocations will be necessary which can accommodate thus locally-intruded "incompatible" deformation. Such process can be achieved by introducing incompatibility tensor field roughly given by the second gradient of the locally introduced strain, e.g., ultimately leading to the kink band formation, corresponding to a band-like pattern in the incompatibility distribution extending plus and minus signs as schematically illustrated in Fig. 2(c)

The "appropriate manner" in the above means the following. In taking account of the incompatibility tensor, e.g., in the hardening law, one must consider the sign in addition to its magnitude. Clearly, the incompatibility distributions extending both positive and negative signs are indispensable to the above-mentioned accommodation processes, without which only the additional hardening may result by doubly counting the contribution. The modulated patterns that emerge in the incompatibility field is thus introduced, whose morphological features such as directionality are

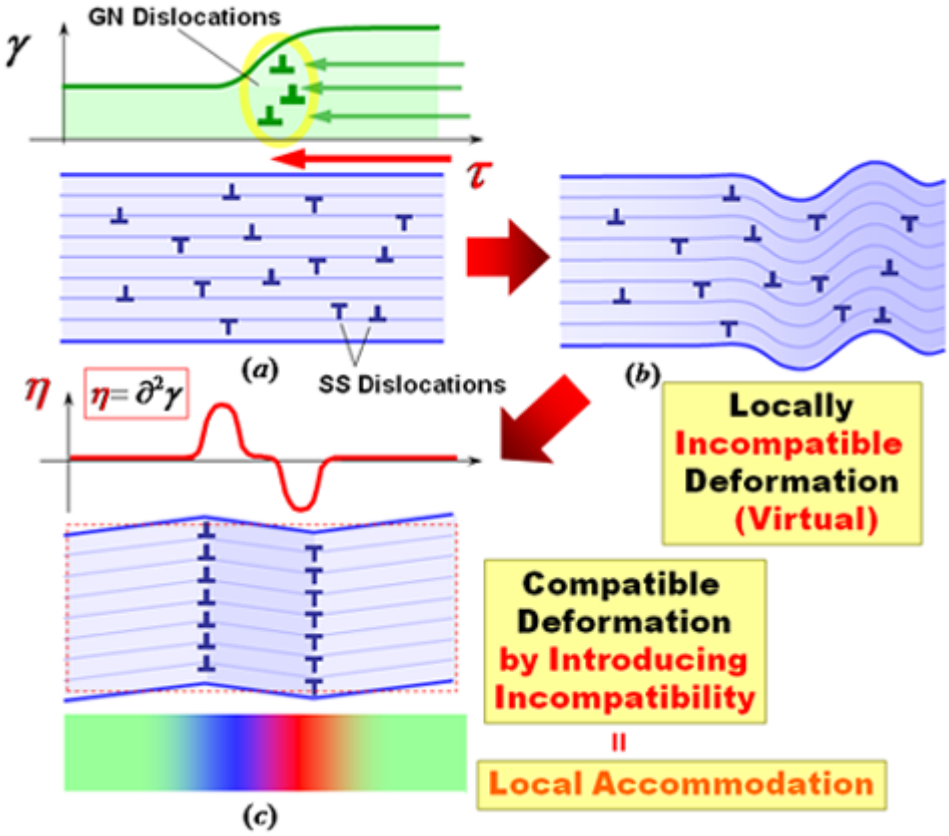

Fig. 2 Schematic indicating an intuitive physical image of incompatibility tensor field, accommodating excessive local deformation via redistribution of dislocations

depending on the crystallography, i.e., crystal orientation and the associated number of active slip systems (Aoyagi and Hasebe 2007).

The above image can also capture another important feature of the incompatibility tensor-based description of inhomogeneous fields in field theory of plasticity. The use of the incompatibility tensor at a certain scale level allows us to account for the underlying "smaller scale"-degree of freedom that is not explicitly considered in the model being used. In the above example, a redistribution of dislocations can be expressed via incompatibility field without introducing or modeling dislocation-degree of freedom explicitly.

3. Theory of interaction fields

3.1 Relative deformation and interaction fields

Let us consider two scales as the simplest case, i.e., coordinates in macro and micro scales, to be denoted by x_i, X_i and $\bar{x}_i, \bar{X}_i$ etc., respectively. Here, $i, j = 1, 2, 3$ in the present paper. All the other quantities referring to the microscale will be expressed by attaching a single "bar" to the

macroscopic counterparts. The quantities in the interaction field, on the other hand, will be similarly expressed by attaching "tilde" instead.

We introduce a relative deformation between the two scales for the purpose of considering field interactions between them in the differential geometrical sense. The relative deformation is defined as the transformation between the line elements dx_i. and $d\bar{x}_i$ for a current configuration (Ikeda 1975), i.e.,

$$d\bar{x}_i = \frac{\partial \bar{x}_i}{\partial x_j} dx_j \equiv A_{ij} dx_j \tag{3}$$

where A_{ij} defines the relative deformation between the two scales. The inverse relationship is given by

$$dx_i = \frac{\partial x_i}{\partial \bar{x}_j} d\bar{x}_j \equiv A^{-1}_{ij} d\bar{x}_j \tag{3a}$$

The above exists only when the determinant of the relative deformation tensor satisfies

$$J_{\text{int}} \equiv \det(A_{ij}) = \left| \frac{\partial \bar{x}_i}{dx_j} \right| \neq 0 \tag{4}$$

This insures the coexistence of the two scales during field evolution.

The transformation of the line vectors before and after deformation is expressed in terms of deformation gradient tensor for both the scales, namely,

$$\begin{cases} dx_i = \dfrac{\partial x_i}{\partial X_j} dX_j \equiv F_{ij} d\, X_j \\ d\bar{x}_i = \dfrac{\partial \bar{x}_i}{\partial \bar{X}_j} d\bar{X}_j \equiv \bar{F}_{ij} d\, \bar{X}_j \end{cases} \tag{5}$$

$$\begin{cases} F_{ij} = \delta_{ij} + \beta_{ij} \\ \bar{F}_{ij} = \delta_{ij} + \bar{\beta}_{ij} \end{cases} \tag{6}$$

Here, $\beta_{ij}, \bar{\beta}_{ij}$ denote distortion tensors for the respective scales. The covariant derivative for the relative deformation is given by,

$$\begin{aligned} D\tilde{X}^k &= d\tilde{X}^k + \Gamma^k_{ij} \tilde{X}^i dx^j + \bar{\Gamma}^k_{ij} \tilde{X}^i d\bar{x}^j \\ &= d\tilde{X}^k + \Gamma^k_{ij} \tilde{X}^i dx^j + \bar{\Gamma}^k_{im} \tilde{X}^i A_{mj} dx^j = d\tilde{X}^k + (\Gamma^k_{ij} + \bar{\Gamma}^k_{im} A_{mj}) \tilde{X}^i dx^j \end{aligned} \tag{7}$$

So if we write the above by expressing

$$D\tilde{X}^k \equiv d\tilde{X}^k + \tilde{\Gamma}^k_{ij} \tilde{X}^i dx^j \tag{8}$$

then, the coefficients of connection in the interaction field are defined as,

$$\tilde{\Gamma}^k_{ij} \equiv \Gamma^k_{ij} + \bar{\Gamma}^k_{im} A_{mj} \tag{9}$$

If we assume affinly interacting deformation fields, the relative deformation tensor is simply expressed by a scalar quantity having a meaning of "scale ratio" characterizing a spatial degree of separation between the two scales, i.e., $A_{ij} = e^{-1}\delta_{ij}$ with $e^{-1} \equiv \bar{l}/l$, multiplied by Kronecker's delta (identity tensor). Considering this simplest case, we rewrite Eq. (9) by using the scale ratio as,

$$\tilde{\Gamma}^k_{ij} = \Gamma^k_{ij} + \bar{\Gamma}^k_{im} \cdot e^{-1}\delta_{mj} = \Gamma^k_{ij} + e^{-1}\bar{\Gamma}^k_{ij} \tag{9a}$$

Substituting $A_{ij} = e^{-1}\delta_{ij}$ into Eq. $(3)_1$, we have a relationship between the two-scale deformation gradient tensors, i.e.,

$$F_{ij} = \delta_{im}\delta_{nj}\bar{F}_{mn} = \bar{F}_{ij} \tag{10}$$

3.3 Expressions for differential geometrical quantities

For the two-scale interaction field, the differentiation is defined as,

$$\tilde{\partial}_i \equiv \frac{\partial}{\partial x_i} + A_{im}\frac{\partial}{\partial \bar{x}_m} = \frac{\partial}{\partial x_i} + e^{-1}\frac{\partial}{\partial \bar{x}_i} \tag{11}$$

Therefore, by definition, the coefficients of connection are given as,

$$\tilde{\Gamma}^k_{ij} = F_{lk}\tilde{\partial}_i F_{jl} = F_{lk}\left(\frac{\partial}{\partial x_i} + e^{-1}\frac{\partial}{\partial \bar{x}_i}\right)F_{jl} = \bar{F}_{lk}\tilde{\partial}_i \bar{F}_{jl} = F_{lk}\frac{\partial F_{jl}}{\partial x_i} + e^{-1}\bar{F}_{lk}\frac{\partial \bar{F}_{jl}}{\partial \bar{x}_i} \tag{12}$$

Thus, we have the total coefficients of connection given as a summation of those in macro and micro fields, i.e.,

$$\tilde{\Gamma}^k_{ij} = \Gamma^k_{ij} + e^{-1}\bar{\Gamma}^k_{ij} \tag{13}$$

which agrees with Eq. (9a).

The skew-symmetric part of the coefficients of connection as in Eq. $(1)_1$ gives torsion tensor in the interaction field.

$$\tilde{S}^k_{ij} = \tilde{\Gamma}^k_{[ij]} = \Gamma^k_{[ij]} + e^{-1}\bar{\Gamma}^k_{[ij]} = S^k_{ij} + e^{-1}\bar{S}^k_{ij} \tag{14}$$

Curvature tensor, on the other hand, is given also by using $\tilde{\Gamma}^k_{ij}$ based on Eq. $(1)_2$. Substituting Eq. (13) into Eq. $(1)_2$, we have,

$$\begin{aligned}
\tilde{R}^{\cdots k}_{lij} &= 2[\tilde{\partial}_{[l}\tilde{\Gamma}^k_{i]j} + \tilde{\Gamma}^k_{[l|m|}\Gamma^m_{i]j}] \\
&= 2[(\partial_{[l} + e^{-1}\bar{\partial}_{[l})(\Gamma^k_{i]j} + e^{-1}\bar{\Gamma}^k_{i]j}) + (\Gamma^k_{[l|m|} + e^{-1}\bar{\Gamma}^k_{[l|m|})(\Gamma^m_{i]j} + e^{-1}\bar{\Gamma}^m_{i]j})] \\
&= 2[\partial_{[l}\Gamma^k_{i]j} + \Gamma^k_{[l|m|}\Gamma^m_{i]j} + e^{-2}(\bar{\partial}_{[l}\bar{\Gamma}^k_{i]j} + \bar{\Gamma}^k_{[l|m|}\bar{\Gamma}^m_{i]j})
\end{aligned} \tag{15}$$

Eq. (15) demonstrates that there explicitly exits the interaction between the two scales for the curvature tensor field. The interaction term, given in the last line of Eq. (15), is expressed by the anti-commutation of sequential differentiations with respect to the two scale coordinates x_i and $\bar{x}_i$. The torsion tensor as in Eq. (14), on the other hand, yields no inter-scale coupling, expressed as a summation of the individual-scale quantities. Note, this is similar to the situation for the Finslerian space-based descriptions of crystalline imperfections (Amari 1962).

The significance of the above results is the following. Explicit inter-scale interactions can come into play only through the curvature tensor field as far as the above framework insists. Since the curvature tensor, as is discussed in the following section, can describe inhomogeneities in any scale levels, we now have a definite way to be able to deal with inter-scale couplings and consequent evolutions of multiple inhomogeneously deforming fields within the framework of continuum mechanics in an explicit manner.

Next, we derive the corresponding continuum mechanics-based expressions to the torsion and curvature tensors obtained above. As shown in Eq. (2), single and double contractions of the torsion and curvature tensors produce two second-rank tensors, called dislocation density and incompatibility tensors, respectively, i.e.,

$$\tilde{\alpha}_{ij} = -\in_{ikl}\partial_k\beta^p_{lj} - e^{-1}\in_{ikl}\bar{\partial}_k\bar{\beta}^p_{lj} = -\in_{ikl}(\partial_k\beta^p_{lj} - e^{-1}\bar{\partial}_k\bar{\beta}^p_{lj}) \tag{16}$$

and

$$\begin{aligned}\tilde{\eta}_{ij} &= \in_{ikl}\in_{jmn}\partial_k\partial_m\varepsilon^p_{ln} + e^{-2}\in_{ikl}\in_{jmn}\bar{\partial}_k\bar{\partial}_m\bar{\varepsilon}^p_{ln} + e^{-1}\in_{ikl}\in_{jmn}(\partial_k\bar{\partial}_m\bar{\varepsilon}^p_{ln} + \bar{\partial}_k\partial_m\varepsilon^p_{ln}) \\ &= \in_{ikl}\in_{jmn}\{\partial_k\partial_m\varepsilon^p_{ln} + e^{-2}\bar{\partial}_k\bar{\partial}_m\bar{\varepsilon}^p_{ln} + e^{-1}(\partial_k\bar{\partial}_m\bar{\varepsilon}^p_{ln} + \bar{\partial}_k\partial_m\varepsilon^p_{ln})\}\end{aligned} \tag{17}$$

It should be noted again, Eq.(16) implies that we cannot take into account any inter-scale coupling explicitly based only on the conventionally and widely used "geometrically-necessary" dislocation densities, whose definition is identical to the dislocation density tensor.

3.4 Extension to multiple scales

The above obtained framework for the interaction field can be readily extended to multiple fields with more than three scales in a straightforward manner. In what follows, Eqs. (16) and (17) are extended to three scale interaction field. In expressing such multiple scales, the direct notation together with sub- or superscripts standing for the scale levels will be used in the place of index notation for simplicity.

Considering two scales, A and B, we rewrite Eqs. (16) and (17) in the direct notation as,

$$\tilde{\boldsymbol{\alpha}} = -curl_B\boldsymbol{\beta}^{pB} - e^{-1}_{BA}curl_A\boldsymbol{\beta}^{pA} \tag{16a}$$

and

$$\tilde{\boldsymbol{\eta}} = curl_B curl_B\boldsymbol{\varepsilon}^{pC} + e^{-2}_{BA}curl_A curl_A\boldsymbol{\varepsilon}^{pA} + e^{-1}_{BA}(curl_B curl_A\boldsymbol{\varepsilon}^{pA} + curl_A curl_B\boldsymbol{\varepsilon}^{pB}) \tag{17a}$$

Let us consider three scales as a first extension. Let the three scales called A, B and C, from small to larger scales, with scale B regarded as a reference. Since the same relationships should hold between arbitrary scale pairs, namely, A and B as well as B and C, the substitution of the curl operation, $curl_B \Rightarrow curl_B + e^{-1}_{BA}curl_A$, is to be made in Eqs. (16a) and (17a). After some algebraic calculations, the three scale expressions of the interaction field are derived as,

$$\bar{\boldsymbol{\alpha}} = -e^{-1}_{BC}curl_C\boldsymbol{\beta}^{pC} - curl_B\boldsymbol{\beta}^{pB} - e^{-1}_{BA}curl_A\boldsymbol{\beta}^{pA} \tag{18}$$

and

$$\tilde{\boldsymbol{\eta}} = e_{BC}^{-2} curl_C curl_C \boldsymbol{\varepsilon}^{pC} + curl_B curl_B \boldsymbol{\varepsilon}^{pB} + e_{BA}^{-2} curl_A curl_A \boldsymbol{\varepsilon}^{pA}$$
$$+ e_{BA}^{-1}(curl_B curl_A \boldsymbol{\varepsilon}^{pA} + curl_A curl_B \boldsymbol{\varepsilon}^{pB}) + e_{BC}^{-1}(curl_B curl_C \boldsymbol{\varepsilon}^{pC} + curl_C curl_B \boldsymbol{\varepsilon}^{pB})$$
$$+ e_{BA}^{-2} \cdot e_{AC}^{-1}(curl_A curl_C \boldsymbol{\varepsilon}^{pC} + curl_C curl_A \boldsymbol{\varepsilon}^{pA}) \tag{19}$$

where $e_{BC}^{-1} \times e_{CA}^{-1} = e_{BA}^{-1}$ is used in the second line of Eq. (19). Note, the product of scale ratios in the third line reads $e_{BA}^{-2} \cdot e_{CA}^{-1} = \dfrac{l_c l_A}{l_B^2}$. Eqs. (18) and (19) can be rearranged in a more compact form,

$$\tilde{\boldsymbol{\alpha}} = e_{BC}^{-1}\tilde{\boldsymbol{\alpha}}^C + \tilde{\boldsymbol{\alpha}}^B + e_{BA}^{-1}\tilde{\boldsymbol{\alpha}}^A \qquad \begin{cases} \tilde{\boldsymbol{\alpha}}^C = -curl_C \boldsymbol{\beta}^{pC} \\ \tilde{\boldsymbol{\alpha}}^B = -curl_B \boldsymbol{\beta}^{pB} \\ \tilde{\boldsymbol{\alpha}}^A = -curl_A \boldsymbol{\beta}^{pA} \end{cases} \tag{20}$$

and

$$\tilde{\boldsymbol{\eta}} = e_{BC}^{-2}\tilde{\boldsymbol{\eta}}^C + \tilde{\boldsymbol{\eta}}^B + e_{BA}^{-2}\tilde{\boldsymbol{\eta}}^A$$

$$\begin{cases} \tilde{\boldsymbol{\eta}}^C = curl_C curl_C \boldsymbol{\varepsilon}^{pC} + e_{CB}^{-1} curl_C curl_B \boldsymbol{\varepsilon}^{pB} + e_{CA}^{-1} curl_C curl_A \boldsymbol{\varepsilon}^{pA} \\ \tilde{\boldsymbol{\eta}}^B = e_{BC}^{-1} curl_B curl_C \boldsymbol{\varepsilon}^{pC} + curl_B curl_B \boldsymbol{\varepsilon}^{pB} + e_{BA}^{-1} curl_B curl_A \boldsymbol{\varepsilon}^{pA} \\ \tilde{\boldsymbol{\eta}}^A = e_{AC}^{-1} curl_A curl_C \boldsymbol{\varepsilon}^{pC} + e_{AB}^{-1} curl_A curl_B \boldsymbol{\varepsilon}^{pB} + curl_A curl_A \boldsymbol{\varepsilon}^{pA} \end{cases} \tag{21}$$

Expressions for multiple fields with more than four scale levels can be similarly derived simply by repeating the same process as the above.

Corresponding matrix expressions to Eqs. $(20)_2$ and $(21)_2$ are given as,

$$\begin{Bmatrix} \tilde{\boldsymbol{\alpha}}^C \\ \tilde{\boldsymbol{\alpha}}^B \\ \tilde{\boldsymbol{\alpha}}^A \end{Bmatrix} = -\begin{bmatrix} curl_C & 0 & 0 \\ 0 & curl_B & 0 \\ 0 & 0 & curl_A \end{bmatrix} \begin{Bmatrix} \boldsymbol{\beta}^{pC} \\ \boldsymbol{\beta}^{pB} \\ \boldsymbol{\beta}^{pA} \end{Bmatrix} \tag{20a}_2$$

and

$$\begin{Bmatrix} \tilde{\boldsymbol{\eta}}^C \\ \tilde{\boldsymbol{\eta}}^B \\ \tilde{\boldsymbol{\eta}}^A \end{Bmatrix} = \begin{bmatrix} curl_C curl_C & e_{CB}^{-1} curl_C curl_B & e_{CA}^{-1} curl_C curl_A \\ e_{BC}^{-1} curl_B curl_C & curl_B curl_B & e_{BA}^{-1} curl_B curl_A \\ e_{AC}^{-1} curl_A curl_C & e_{AB}^{-1} curl_A curl_B & curl_A curl_A \end{bmatrix} \begin{Bmatrix} \boldsymbol{\varepsilon}^{pC} \\ \boldsymbol{\varepsilon}^{pB} \\ \boldsymbol{\varepsilon}^{pA} \end{Bmatrix} \tag{21a}_2$$

3.5 Some remarks on multiple scale formalism

The off-diagonal components in the curl matrices, e.g., those of Eq. (21a), represent inter-scale field couplings without which independency of each scale is rationalized. The curl matrix for incompatibility Eq. (21a) is asymmetric in general because of the asymmetry of the scale ratios, i.e., $e_{CB}^{-1} \neq e_{BC}^{-1}$, $e_{CA}^{-1} \neq e_{AC}^{-1}$, $e_{BA}^{-1} \neq e_{AB}^{-1}$, and also due to a loss of information caused by coarse-graining,

e.g., during the alternating curl operations with respect to the distinct scales. A pair of the off-diagonal components in the curl matrix can become symmetric only when the two scales coincide. The loss of information can be measured by the commutation relation of the curl operations, i.e., exchange of the order of curl operations.

$$[curl_I, curl_J]_{\text{int}} \equiv curl_I, curl_J \boldsymbol{\varepsilon}^{pJ} - curl_J curl_I \boldsymbol{\varepsilon}^{pI} \tag{22}$$

where, in the present case, the subscripts I and J express either of A, B or C. On the other hand, the non-commutativity of the curl operations with respect to the distinct two scales measures the strength of the field interaction, i.e., the measure of inter-scale correlation.

$$\{curl_I, curl_J\}_{mes} \equiv curl_I, curl_J \boldsymbol{\varepsilon}^{pJ} - curl_J curl_I \boldsymbol{\varepsilon}^{pI} \tag{23}$$

For the same distribution of $\boldsymbol{\varepsilon}^p$, we generally have $[curl_I, curl_J]_{\text{int}} = 0$ even when spatially different scales are considered, making the curl matrix symmetric if there is no information loss.

In real situations, e.g., those associated with the polycrystalline plasticity as will be discussed in Part II of the paper, we expect to have $[curl_I, curl_J]_{\text{int}} \neq 0$ for the assumed scales A, B and C, corresponding to (A) dislocation substructures, (B) intra-granular and (C) trans-granular inhomogeneities, respectively, because of their distinct physical and geometrical origins as well as the change rates of the field evolutions. Their origins are the following; i.e., collective behavior of dislocations and the concomitant patterning for scale A (e.g., with cellular morphology), and accommodations of deformation for scale B and C. Moreover, the scale B yields modulated distributions having more or less directionalities in stress and strain fields due to accommodation of deformation based on intra-granular crystallography, i.e., crystal orientation and associated redistribution of dislocations (e.g., with lamellar morphology), whereas the scale C exhibits that associated with trans-granular accommodation of inhomogeneity driven by the collective behavior of crystal grains which does not yield modulated patterns in general (e.g., with nearly random morphology reflecting the randomness of the composing grains' orientation distribution).

It is noteworthy that the above formalism can be readily extended to the space-time framework based on which the coupling or interaction among distinct "temporal" scales are explicitly dealt with simultaneously. This is also intriguing as well as challenging open question that we must face in accomplishing the multiscale modeling of materials. The temporal aspects of the inter-scale coupling is closely related with the evolutionary features of the multiple fields of interests, which are partially involved in the constitutive descriptions to be modeled in the analysis.

Also to be noted is that the present formalism is not confined to continuum mechanics but can be applied to discrete pictures of dislocations and defects, e.g., those based on discrete dislocations as well as atomistics as far as the incompatibility tensor can be evaluated. For discrete dislocation representations, the dislocation density tensor can be directly evaluated via (Zbib *et al.* 2004)

$$\alpha_{ji} = \sum_{s=1}^{N_s} \frac{l_s}{V} b_{si} \xi_{sj}, \quad \boldsymbol{\alpha} = \sum_{s=1}^{N_s} \frac{l_s}{V} \boldsymbol{b}_s \otimes \boldsymbol{\xi}_s,$$

given a configuration of dislocation segments, from which all the components in the incompatibility tensor are explicitly calculated. Here, $\boldsymbol{b}_s, \boldsymbol{\xi}_s$ represent Burgers vector and the local line tangent direction, respectively, while s stands for a dislocation segment, l_s the segment length, N_s the total number of dislocation segments, and V the volume of the representative volume element assumed.

4. Implementation of interaction field into constitutive framework

4.1 Constitutive framework

The above-constructed interaction field framework is implemented into the crystalline plasticity model through the strain gradient terms (Aoyagi and Hasebe 2007). A constitutive model applicable both to FCC and BCC metals have been proposed by the author based on statistical mechanics-based dislocation dynamics. The explicit form is given by,

$$\begin{cases} \dot{\gamma}^{(\alpha)} = \dot{A}_{SR}\tau'^{(\alpha)}\left[\left|\tau'^{(\alpha)}\right|B_{SR}\exp\left\{1-\left(\dfrac{\tau'^{(\alpha)}}{K^{(\alpha)}}\right)^{p}\right\}^{q}+C_{SR}\right]^{-1} \\ \tau'^{(\alpha)} \equiv \langle\, \tau^{(\alpha)} - \tau^{*(\alpha)}_{Peierls}\rangle - \Omega^{(\alpha)} \end{cases} \tag{24}$$

with

$$\dot{A}_{SR} = \rho_m b L \upsilon^{*}, B_{SR} = \frac{\Delta G_0^{disloc}}{kT}, C_{SR} = \frac{BL\upsilon^{*}}{b} \tag{24a}$$

where $K^{(\alpha)}$ and $\Omega^{(\alpha)}$ are drag and back stress, respectively, responsible for isotropic and kinematic types of hardening. In Eq. (24a), $\rho_m, L, \upsilon^{*}, b$ are mobile dislocation density, mean flying distance of dislocations, the Debye frequency, the magnitude of Burgers vector and the damping coefficient due to, e.g., phonon drag, respectively, and $\Delta G_0^{disloc} \equiv \mu(T) b^3 g_0^{disloc}$ stands for the activation energy for dislocation processes at T = 0K with g_0^{disloc} being the normalized one and $\mu(T)$ the temperature dependent shear modulus. For BCC metals, we can set $C_{SR} = 0$, whereas for FCC we normally assume $\tau^{*(\alpha)}_{Peierls} \simeq 0$. The exponents p and q in Eq. $(24)_1$ are the parameters specifying the thermal obstacle of interest, provided $0 \le p \le 1$ and $1 \le q \le 2$. In the above case, a pair of values $p = 1/2$, $q = 3/2$ is used for representing dislocation processes. Furthermore in Eq. $(24)_1$, $\langle \mathrm{O} \rangle \equiv (|\mathrm{O}| + \mathrm{O})/2$ represents the Mackauley parenthesis, with $\tau^{*(\alpha)}_{Peierls}$ expressing the effective stress for Peierls overcoming process given by,

$$\tau^{*(\alpha)}_{Peierls} = \left[1-\left(\frac{kT}{g_0^{Peierls}\mu b^3}\ln\frac{\dot{\gamma}_{0Peierls}}{\dot{\gamma}^{(\alpha)}}\right)^{1/q_{Peierls}}\right]^{1/P_{Peierls}} \tag{25}$$

where $g_0^{Peierls}$, $\dot{\gamma}_{0Peierls}, p_{Peierls}$ and $q_{Peierls}$ are parameters for the thermal activation process via Peierls overcoming event of dislocations.

The hardening evolution models are introduced through drag stress $K^{(\alpha)}$ and back stress $\Omega^{(\alpha)}$ (Hasebe *et al.* 1998b) given respectively by,

$$\dot{K}^{(\alpha)} = Q_{\alpha\beta}H(\gamma)\left|\dot{\gamma}^{(\beta)}\right| \text{ and } \dot{\Omega}^{(\alpha)} = -A_{cell}\{\langle d^{*}_{cell} - \bar{x}^{(\alpha)}_{N}\rangle + \alpha\}^{-2} \tag{26}$$

where $H(\gamma)$ represents hardening modulus for a referential stress-strain curve. Hardening ratio $Q_{\alpha\beta}$ is used to evaluate the effective cell size which characterizes the average size of dislocation substructure like cell, given by

$$d_{cell} = k\left(\frac{1}{N}Q_{\alpha\beta}Q_{\alpha\beta}\right)^{-\frac{1}{2}} \text{ and } d_{cell}^{(\alpha)} = k\left(\sum_{\beta=1}^{N} Q_{\alpha\beta}Q_{\alpha\beta}\right)^{-\frac{1}{2}} \tag{27}$$

where k represents the initial cell size normally coinciding with a fraction of the initial grain size. For the evolution equation of the back stress $Q_{\alpha\beta}$, $d_{cell}^{*} \equiv d_{cell}/2$ and $\bar{x}_N^{(\alpha)}$ is the mean moving distance of dislocations evaluated by multiplying $l^{*} \equiv 1/(\rho_m b)$ with $\dot{\gamma}^{(\alpha)}$.

4.2 Hardening law and field theoretical strain gradient terms

The hardening ratio $Q_{\alpha\beta}$, in Eq. $(26)_1$ through which the contributions of $\tilde{\alpha}_{ij}$ and $\tilde{\eta}_{ij}$ are accounted for, is given by,

$$Q_{\alpha\beta} = f_{\alpha\kappa} S_{\kappa\beta} + \delta_{\alpha\beta}\{1 + F(\tilde{\alpha}^{(\beta)}; \tilde{\eta}^{(\beta)})\} \tag{28}$$

where $f_{\alpha\kappa}$ represents dislocation interaction matrix, and $S_{\kappa\beta}$ expresses history matrix further given as an increasing function of plastic work done by the effective stress that responsible for dislocation processes. No summation is taken in the last term in the right-hand side of Eq. (28). Here, $F_k(\tilde{\alpha}_k^{(\beta)}; \tilde{\eta}_k^{(\beta)}) \equiv F_k \tilde{\alpha}_k^{(\beta)} + F_k \tilde{\eta}_k^{(\beta)}$ expresses the field theoretical "strain gradient terms" given respectively as (Aoyagi and Hasebe (2007)),

$$F(\tilde{\alpha}^{(\alpha)}) = k \cdot d_{cell}^{\alpha(\alpha)^{-1}} = \frac{k}{p_\alpha}\left(\frac{|\tilde{\alpha}^{(\alpha)}|}{b}\right)^{1/2} \tag{29}$$

$$F(\tilde{\eta}^{(\alpha)}) = k \cdot d_{cell}^{\eta(\alpha)^{-1}} = \mathrm{sgn}(\tilde{\eta}^{(\alpha)}) \cdot \frac{k}{p_\eta}\left(\frac{l_{defect}}{b}|\tilde{\eta}^{(\alpha)}|\right)^{1/2} \tag{30}$$

where p_α, p_η are coefficients related with the contributions of $\tilde{\alpha}_k^{(\beta)}$ and $\tilde{\eta}_k^{(\beta)}$ to the change in the effective cell size d_{cell}, while l_{cell} represents the characteristic length of the defect field considered, e.g., $l_{defect} = b$ for dislocation dipoles and $l_{defect} \sim 10^{-6}$ for dislocation substructures like cells. Here $\tilde{\alpha}_k^{(\beta)}$ and $\tilde{\eta}_k^{(\beta)}$ are the resolve components of $\tilde{\alpha}_{ij}$ and $\tilde{\eta}_{ij}$, respectively, defined as,

$$\tilde{\alpha}_k^{(\alpha)} = (t_i^{(\alpha)} s_j^{(\alpha)} + s_i^{(\alpha)} s_j^{(\alpha)})\tilde{\alpha}_{ij} \text{ and } \tilde{\eta}_k^{(\alpha)} = s_i^{(\alpha)} t_j^{(\alpha)} \tilde{\eta}_{ij} \tag{31}$$

where $t_i^{(\beta)} = \in_{ijk} s_j^{(\beta)} m_k^{(\beta)}$ with $s_j^{(\beta)}, m_k^{(\beta)}$ being the unit vectors in the slip direction and slip plane normal, respectively. Note, that the first and second terms of $\tilde{\alpha}_k^{(\beta)}$ respectively correspond to the edge and screw components of dislocation density.

The explicit forms of Eqs. (29) and (30) were obtained as follows. Since the hardening ratio $Q_{\alpha\beta}$ physically dictates the inverse of the effective cell size, in the present context as understood from Eq. (27), characterizing the mean dislocation free path, the strain gradient terms to be introduced should have the same dimensionality, bearing the effect of either enhancing or reducing it. For the dislocation density, we can evaluate the mean spacing of dislocations via

$$\bar{l}_{disloc}^{(\alpha)} = \left(\frac{1}{b}|\tilde{\alpha}^{(\alpha)}|\right)^{-1/2} \tag{32}$$

since $(1/b)|\tilde{\alpha}^{(\alpha)}|$ counts "geometrically-necessary" types of dislocation density. Assuming the proportionality between the cell size and $\bar{l}_{disloc}^{(\alpha)}$ based on empirical facts, i.e.,

$$\Delta_\alpha d_{cell}^{(\alpha)} = p_\alpha \cdot \bar{l}_{disloc}^{(\alpha)} \tag{33}$$

with p_α being the proportionality factor, we arrive at Eq. (29).

The same is true also for the incompatibility tensor, except one additional parameter l_{defect} and the sign of $\tilde{\eta}^{(\alpha)}$. The former is to be introduced for the dimensionality reason, while the latter is to take account of the accommodation ability of the quantity, dictating how the dislocations are redistributed to relax the excessive deformation as described in section **2.2**, Hence, we have

$$\Delta_\eta d_{cell}^{(\alpha)} \equiv p_\eta \cdot \bar{l}_{defect}^{(\alpha)} = p_\eta \cdot \mathrm{sgn}(\tilde{\eta}^{(\alpha)}) \left(\frac{l_{defect}}{b} \left| \tilde{\eta}^{(\alpha)} \right| \right)^{-1/2} \tag{34}$$

By combining the contributions given by Eqs. (33) and (34) to the effective cell size evolution, we ultimately have,

$$Q_{\alpha\beta} = \delta_{\alpha\beta} + f_{\alpha\kappa} S_{\kappa\beta} + \delta_{\alpha\beta} k \{ \Delta_\alpha d_{cell}^{(\alpha)\,-1} + \Delta_\eta d_{cell}^{(\alpha)\,-1} \}$$

leading to the final expression in Eq. (28). Note, the effect of evaluation method of the derivative for obtaining $F(\tilde{\eta}^{(\alpha)})$ distribution is extensively discussed in (Aoyagi *et al*. 2008).

5. Conclusions

This paper describes in detail a concept and the associated derivation process of the interaction fields applicable to multiple scale problems based on field theory of plasticity. Relative deformation between two distinct scales, e.g., macro and micro fields, are considered based on which all the other differential geometrical quantities, i.e., the coefficients of connection, torsion tensor and curvature tensor, are derived. Thus obtained two-scale interaction formalism is extended to multiple scales with more than three levels. Demonstrated are the explicit coupling exists in the curvature tensor field, equivalent to incompatibility tensor field, whereas no coupling in the torsion, i.e., dislocation density, tensor field. The interaction fields are implemented into a crystal plasticity-based constitutive equation through which we can tackle multiscale problems in the light of interactions in an explicit manner.

References

Amari, S. (1962), "A theory of deformations and stress of ferromagnetic substances by Finsler geometry", *RAAG Memoirs*, **3**, 257-278.

Aoyagi, Y. and Hasebe, T. (2007), "New physical interpretation of incompatibility and application to dislocation substructure evolution", *Key Engineering Materials*, **340-341**, 217-222

Aoyagi, Y., Hasebe, T., Chen, J.S. and Guan, P.C. (2007)(APCOM'07)

Benssousan, A., Lions, J.-L. and Papanicoulau, G. (1978), *Asymptotic Analysis for Periodic Structures*, North-Holland, Amsterdam-New York-Oxford.

Chen, Z.Z., Kioussis, N., Ghoniem, N. and Hasebe, T. (2008), "Lubricant effect of copper nano-clusters on dislocation core in α-Fe", *Physical Review B.*, **77**-1, 014103

Epstein, M. and Elzanowski, M. (2007), *Material Inhomogeneities and their Evolution*, Springer.

Hasebe, T., Kumai, S. and Imaida, Y. (1999), "Impact behavior of FCC metals with pre-torsion strains", *Mater. Process. Technol.*, **85**, 184-187.

Hasebe, T. (2004a): "Continuum description of inhomogeneously deforming polycrystalline aggregate based on field theory", *Mesoscopic Dynamics of Fracture Processes and Materials Strength* (*Proc. IUTAM Symp.*), Eds. H. Kitagawa, Y. Shibutani, Kluwer, 381-390.

Hasebe, T. (2004b), "Field theoretical multiscale polycrystal plasticity", *MRS-J*, **29**(8), 3619-3624.

Hasebe, T. (2006), "Multiscale crystal plasticity modeling based on field theory", *CMES*, **11**(3), 145-155.

Hasebe, T. (2009), "Field theory-based description of interaction field for multiple scales: Part II -Application-," *Interaction Multiscale Mech., An Int. J.*, **2**(1), 15-30.

Ikeda, S. (1975), "Prolegomena to applied geometry", Maha-shobo (in Japanese).

Kondo, K. (1955), "Non-Riemannian geometry of imperfect crystals from a macroscopic", *RRAG Memoirs*, **1**, D-I, 458-469.

Terada, K. and Kikuchi, N. (2001), "A class of general algorithms for non-linear multi-scale analyses of heterogeneous media", *Comput. Methods Appl. Mech. Eng.*, **190**, 5427-5464.

Zbib, H.M., Hiratani, M. and Shehadeh, M. (2004), "Multiscale discrete dislocation dynamics plasticity," in *Continuum Scale Simulation of Engineering Materials* (eds. Raab, D., Roters, F., Barlat, F. and Chen, L.-Q.), 543-560, Wiley-VCH.